Simultaneous deposition of Au nanoparticles during flame synthesis of TiO_2 and SiO_2

L. Mädler, W.J. Stark, and S.E. Pratsinis[a)]
Particle Technology Laboratory, Department of Mechanical and Process Engineering, Eidgenössische Technische Hochschule (ETH) Zürich, CH-8092 Zürich, Switzerland

(Received 2 July 2002; accepted 14 October 2002)

Nanostructured gold/titania and gold/silica particles with up to 4 wt% Au were made by a single-step process in a spray flame reactor. Gold(III)-chloride hydrate and titania- or silica-based metalorganic precursors were mixed in a liquid fuel solution, keeping concentrations in the flame and overall combustion enthalpy constant. The powders were characterized by x-ray diffraction, transmission electron microscopy, Brunauer–Emmett–Teller, and ultraviolet–visible analysis. The titania or silica specific surface area and the crystalline structure of titania were not affected by the presence of gold in the flame. Furthermore the size of the gold deposits was independent of the metal oxide support (TiO_2 or SiO_2) and its specific surface area (100 and 320 m^2/g, respectively). The gold nanoparticles were nonagglomerated, spherical, mostly single crystalline, and well dispersed on the metal oxide support. Depending on the Au weight fraction (1, 2, and 4 wt%) the Au nanoparticles' mass mean diameter was 3, 7, and 15 nm, respectively, on both titania and silica. The particles showed surface plasmon absorption bands in the ultraviolet–visible region, which is typical for nano-sized gold. This absorption band was red shifted in the case of the titania support, while no shift occurred with the silica support.

I. INTRODUCTION

The preparation of fine metal particles on oxides plays a crucial role in determining product properties of a wide range of materials used in optics, catalysis, electronics, and ceramics. In general, such metal particles are prepared by wet precipitation of the metal on a support and by co-precipitation or by two-step processes in which metal and ceramic supports are made separately, such as sputtering, chemical vapor deposition, and grafting or impregnation.[1–4]

A particularly attractive route for synthesis of highly pure materials (e.g., lightguides for telecommunication) is flame aerosol technology, which can also be used for synthesis of metal–ceramic nanoparticles.[5] Direct aerosol synthesis of gold nanoparticles (aerosol) was introduced recently by Magnusson *et al.*[6] and Nakaso *et al.*[7] using an evaporation/condensation process in a tube furnace reactor. They investigated sintering and restructuring mechanisms of gold particles theoretically and experimentally. The mobility diameter of the gold particles was controlled from about 10 to 30 nm with the temperature of the furnace. A one-step aerosol synthesis of a supported noble metal on a metal oxide (Pt/TiO_2) was proposed by Johannessen and Koutsopoulos[8] who fed and simultaneously combusted Ti-isopropoxide and platinum acetylacetonate [$Pt(acac)_2$] vapors in a quench-cooled flame reactor. The product powder consisted of aggregated titania with Pt particles of about 2 nm. However, when this vapor flame approach was used, all precursors had to be evaporated before entering the reaction zone (vapor flame), resulting in a low production rate (tens of milligrams per hour) because of the low vapor pressure and volatility of the noble metal precursor [$Pt(acac)_2$].

Spraying and combusting a liquid precursor in a flame can substantially increase the nanoparticle production rate.[9] Besides the possibility of generating the metal and the ceramic support at the same time, flame technology, and especially the spray flame processes, can provide virtually all kinds of support materials: metal oxides (e.g., alumina, silica, and titania,[5,10] without deposition of metals), mixed metal oxides (e.g., spinel, mullite, and strontium aluminosilicate[11]) or metal oxide composites (e.g., silica/titania[12]).

For this paper, one-step synthesis of Au/TiO_2 or Au/SiO_2 particles by flame spray pyrolysis was investigated. These two distinctly different supports were selected to better understand the possible role of substrate on Au nanoparticles formation pathways as a function of precursor concentration at constant combus-

a)Address all correspondence to this author.
e-mail: pratsinis@ptl.mavt.ethz.ch

tion enthalpy. Crystallite sizes were determined by x-ray diffraction (XRD) (Rietveld method). Microscopy images were used to determine the gold particle size while nitrogen adsorption was used to measure the specific surface area. Formation of Au particles was investigated and found to be independent of the substrate carrier oxide. The ultraviolet–visible (UV–vis) spectrum of these Au/TiO_2 and Au/SiO_2 particles was also investigated.

II. EXPERIMENTAL

The flame spray pyrolysis (FSP) reactor used in this study was described in detail by Mädler *et al.*[13,14] The premixed supporting methane/oxygen (CH_4 = 1.5 l/min, O_2 = 3.2 l/min) flamelets were replaced by a concentric flamelet ring, ensuring complete radial homogeneity. Furthermore, the present reactor was water cooled to avoid any evaporation of the precursor within the liquid feed lines. The liquid precursor was fed by a syringe pump with a rate of either 3.0 or 3.1 ml/min and was dispersed by 3 l/min of oxygen (Pan Gas, Luzern, Switzerland) into fine droplets by the gas-assist nozzle (pressure drop, 1.5 bar). Additional oxygen (5 l/min) was supplied by an outer sheath flow to assure enough oxidant for complete conversion of the reactants. The powder was collected on a glassfiber filter (GF/A Whatman, Kent, United Kingdom), 150 mm in diameter. The filter was placed in a water-cooled holder 400 mm above the nozzle. The cooling of the filter housing ensured an off-gas temperature below 200 °C.

For the titania support, titanium(IV)-isopropoxide (TTIP; Aldrich, Buchs, Switzerland; 97%) in xylene was used. The precursor was fed into the reactor to achieve a titania production rate of 2×10^{-3} mol/min. In the case of silica, tetraethyl-orthosilicate (TEOS; Aldrich; 98%) was used as precursor. To ensure identical metal concentrations of 0.68 M and an identical combustion enthalpy of −100 kJ/min for both precursors, the TEOS precursor was mixed with a solution of 10 vol% iso-octane in xylene and delivered at 3.1 ml/min to achieve a silica production (or TEOS delivery) rate of 2×10^{-3} mol/min. Acetonitrile (2.6 vol%) containing different amounts of gold(III)-chloride hydrate (Fluka, Buchs, Switzerland; purum, 50% Au) was added to these solutions, resulting in gold/metal oxide ratios of 0, 0.5, 1, 2, and 4 wt%.

High-resolution transmission electron microscopy (HRTEM) pictures of the powders were taken with a Philips CM30ST (300 kV) (Amsterdam, The Netherlands) microscope. Gold particles were counted and size classified from the HRTEM pictures using the software Optimas (Media Cybernetics L.P.). The XRD patterns were recorded [Bruker, AXS D8 Advance (40 kV, 40 mA)] and used to obtain crystallite sizes (d_{XRD}) and individual mass fractions based on the fundamental parameter approach and the Rietveld method[15] with the structural parameters of gold (Inorganic Crystal Structure Database [ICSD] Coll. Code: 44362; FIZ Karlsruhe, Germany), TiO_2-anatase (ICSD Coll. Code: 63711), and TiO_2-rutile (ICSD Coll. Code: 44881). A linear background was used when matching the XRD patterns. The bulk optical absorption spectra were recorded in the Kubelka–Munk mode with an ultraviolet-visible-near-infrared spectrometer (Cary 500, Varian). The Brunauer–Emmett–Teller (BET) powder specific surface area, was measured by nitrogen adsorption at 77 K (Micromeritics Gemini 2375; Norcross, GA) after degassing the sample for at least 1 h at 150 °C in nitrogen.

III. RESULTS

Precursor solutions were sprayed and ignited by the supporting flamelet ring, resulting in a stable spray flame (visible height, 10 cm) producing 9.8 g/h TiO_2 and 7.3 g/h SiO_2. The specific surface areas were 100 m^2/g for titania and 320 m^2/g for silica, independent of the Au content. The addition of the gold precursor had no influence on the flame appearance, ceramic precursor solubility, or specific surface area. Pure titania and the silica powders had a white appearance while the addition of gold changed their color into violet/brownish. The HRTEM images in Fig. 1 show examples of the gold cluster deposits on (a) titania (1 wt% Au) and (b) silica (4 wt% Au). The gold particles can be distinguished by their sharp contrast. They are mostly spherical in shape and well distributed on the surface of the metal oxide support.

Figure 2 shows an example of the XRD pattern of a titania powder prepared with 4 wt% gold. The size of the gold crystallites on titania was obtained by subtracting (1) the corresponding XRD pattern from (2) pure titania (0 wt% Au). After subtraction (1 − 2), the gold structure can be clearly seen (vertical lines represent the diffraction peaks of cubic gold, Fig. 2). Furthermore, there is no indication of any crystal phase change of the titania. This method was used to determine the gold crystallite size for 1, 2, and 4 wt% Au on titania (Fig. 3), resulting in average crystallite sizes of 3.8, 8.6, and 14.8 nm, respectively. To evaluate the gold content of the sample, the spectra were regressed to the anatase, rutile, and cubic gold patterns. Figure 4 shows an example for 4 wt% Au resulting in 71.4 wt% anatase, 24.7 wt% rutile, and 3.9 wt% gold. The as-obtained gold crystallite size is in good agreement with the one obtained by subtracting the pattern of pure titania from that of Au/TiO_2 (16.1 and 14.8 nm, respectively). The estimated gold weight fractions are in good agreement with the nominal values of 0, 1, and 2 wt% (0.1, 1.1, and 2.1 wt%, respectively). The anatase fraction was 73, 78, 78, and 71 wt% for 0, 1, 2, and 4 wt% gold, respectively. This is in agreement with the difference spectra in Fig. 2.

https://doi.org/10.1557/JMR.2003.0017

A similar procedure was applied for gold/silica. Silica is x-ray amorphous and was considered by a pseudo-Voigt function in the regression procedure. An example of the regressed XRD pattern of 4 wt% gold on silica is shown in Fig. 5. Using this approach, crystallite sizes for 1, 2, and 4 wt% gold on silica were obtained as shown in Fig. 6. To check the XRD results, the gold particles in the HRTEM images were counted and size classified as shown in Fig. 7 (4 wt% Au on silica). The count mean diameter d_N of the gold size distribution was 9 nm with a standard deviation of 2.3 nm, while the mass mean diameter was 10.6 nm and the count geometric standard deviation, σ_g, was 1.27 from 190 particles.[16]

Figure 8 compares the gold crystallite sizes on titania and silica. Even though the support materials have very different specific surface areas (titania, 100 m^2/g; silica, 320 m^2/g), the gold crystallite particles have comparable sizes when deposited at the same weight content. Doubling the weight content (from 1 to 2 wt% Au), and therefore doubling the concentration of the gold in the flame,

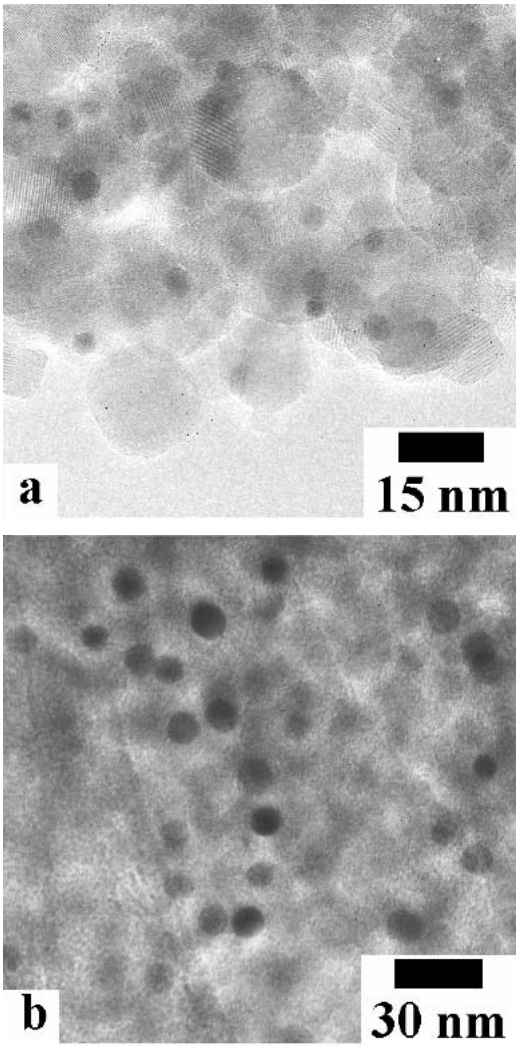

FIG. 1. TEM pictures of (a) 1 wt% Au on titania and (b) 4 wt% Au on silica. The gold particles (dark dots) are mostly spherical and well dispersed on the metal oxide support. The gold particles of 1 wt% Au/TiO_2 are much smaller than those of 4 wt% Au/SiO_2.

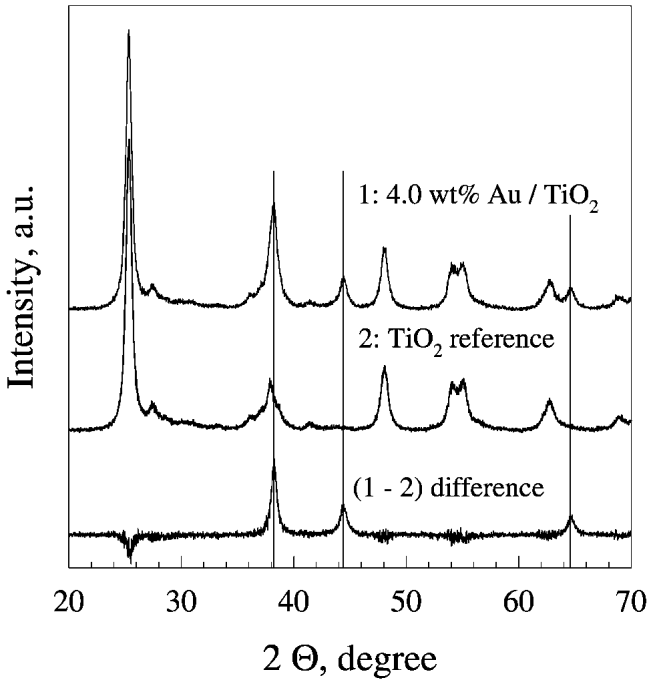

FIG. 2. XRD patterns of (1) 4 wt% Au/TiO_2 and (2) pure TiO_2. The (1–2) difference of the spectrum reveals clearly the gold structure (vertical lines represent diffraction peaks of cubic gold), indicating also that the presence of gold does not affect the phase composition of titania.

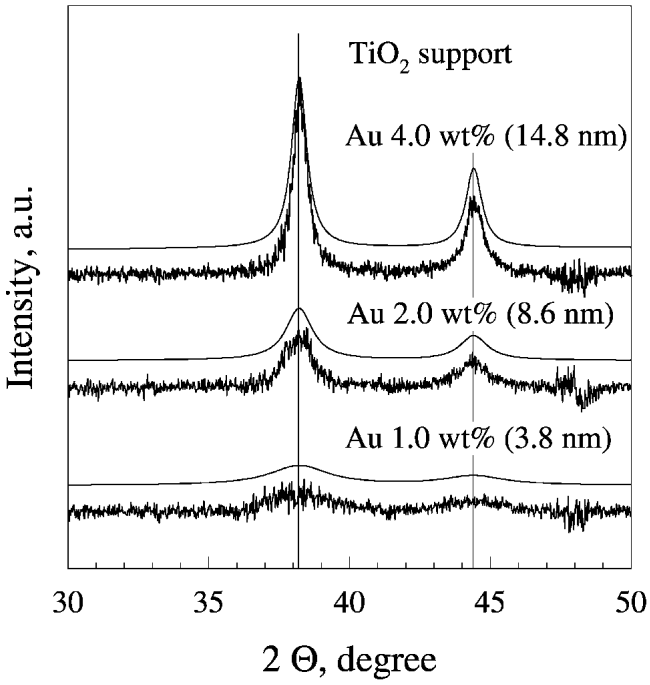

FIG. 3. The XRD difference patterns as obtained in Fig. 2 for 1, 2, and 4 wt% Au on titania. The size of the gold crystallites was obtained by regressing the (1–2) difference pattern of Fig. 2 to that of cubic gold.

roughly doubles the gold particle size. The same trend is found by increasing the concentration of gold again by a factor of 2 from 2 to 4 wt% Au.

Small gold clusters show a very intense surface plasmon absorption band in the visible part of the spectrum, especially when well separated in a colloidal suspension.[17] The flame-made particles exhibit these bands as shown in Fig. 9 for various weight fractions of gold on titania. The height of the absorption band is proportional to the amount of gold on the titania. The maximum of the plasmon absorption band for the Au/TiO_2 powders is at 540 nm and does not vary with the amount of gold on the support. The plasmon band of the Au/TiO_2 composite is red-shifted by 18 ± 2 nm compared to the expected peak position at 522 nm for unsupported gold.[17] The flame-made silica/gold composite and a calculated unsupported gold cluster (Mie Theory by Bohren and Huffman[18] using the refractive index of gold given by Johnson and Christy[19]) did not show a red shift of the plasmon absorption (Fig. 10). This agrees well with the absence of large Au particles in the XRD measurements, which would result in a peak shift to longer wavelengths.

IV. DISCUSSION

The concentration of titania or silica in the flame is much higher than that of gold. Both metal oxides nucleate extremely fast. Particles of the oxide support quickly grow by condensation, coagulation, and sintering as already shown.[5] The low concentration of gold leads to late nucleation of the Au particles with little coagulation as its size distribution is narrower ($\sigma_g = 1.27$) than that of

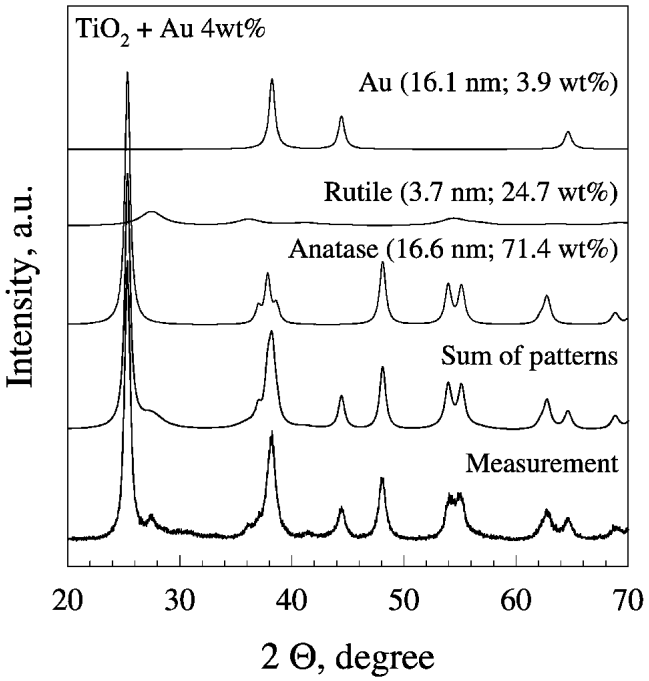

FIG. 4. The 4 wt% Au on titania XRD pattern and its reconstruction using the structural information of anatase, rutile, and gold. The reconstructed pattern resulted in a crystal size of 16.1 nm, which is in good agreement with the regressed difference pattern (14.8 nm, Fig. 3). The evaluated gold content (3.9 wt%) of the powder is in good agreement with the prepared solution (4 wt% Au).

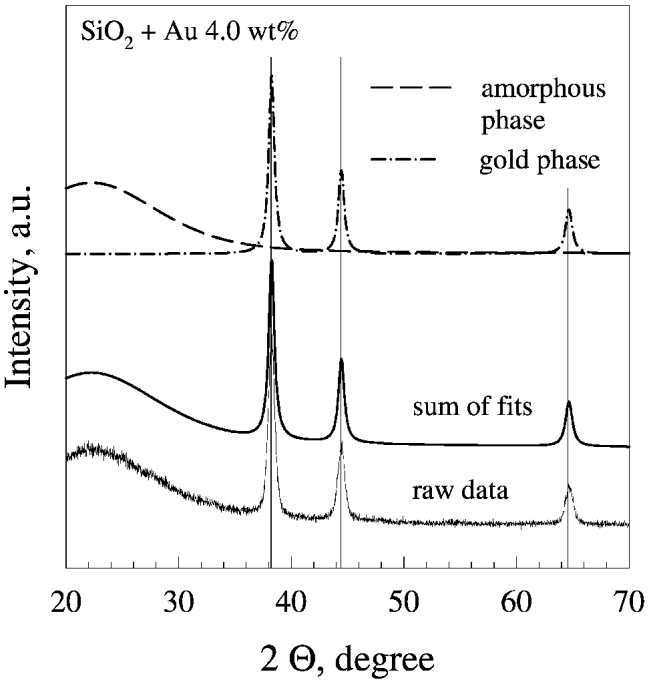

FIG. 5. XRD pattern of 4 wt% Au/SiO_2. The silica was represented by a pseudo-Voigt function regressing the amorphous part of the spectrum and the gold by the cubic Au crystal structure (vertical lines).

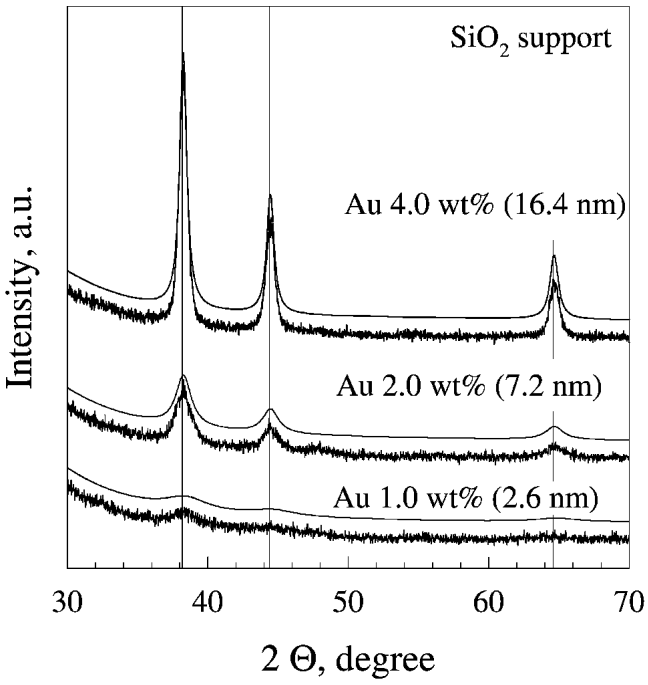

FIG. 6. Crystallite sizes for 1, 2, and 4 wt% Au on silica obtained by regressing the XRD patterns of the as-prepared powder according to Fig. 5.

the self-preserving distribution (σ_g = 1.45) for coagulation.[5] The formation of gold oxides is unfavorable, and gold may be thought of as an ideal system to study the deposition of a metal on a support metal oxide.

In the study by Magnusson *et al.*[6] a gold aerosol (10 nm in size) was thermally treated in a furnace reactor.[6] They obtained spherical, mainly single-crystalline gold particles at temperatures above 745 °C.

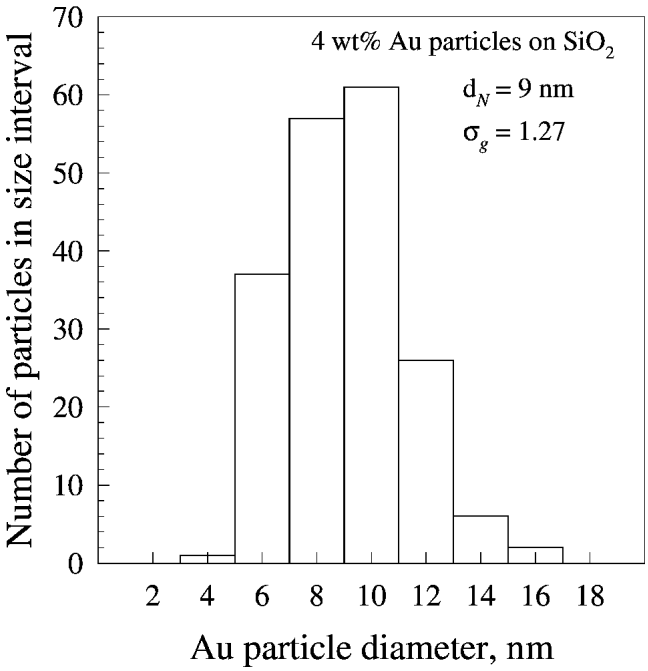

FIG. 7. Number size distribution of gold nanoparticles on silica (4 wt% Au) as determined by TEM image counting.

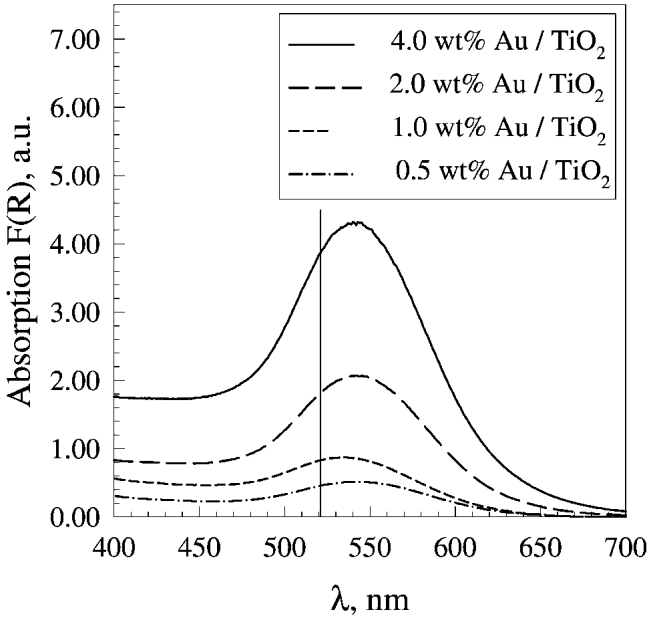

FIG. 9. UV-vis spectra of 0.5, 1, 2, and 4 wt% Au on titania. Different amounts of gold loadings do not change the peak location of the plasmon band, indicating that the gold crystallites are smaller than 20 nm. The peak position of the spectra (540 nm) is red shifted compared to the pure gold plasmon peak (vertical line), indicating a weak interaction between the gold and the support.

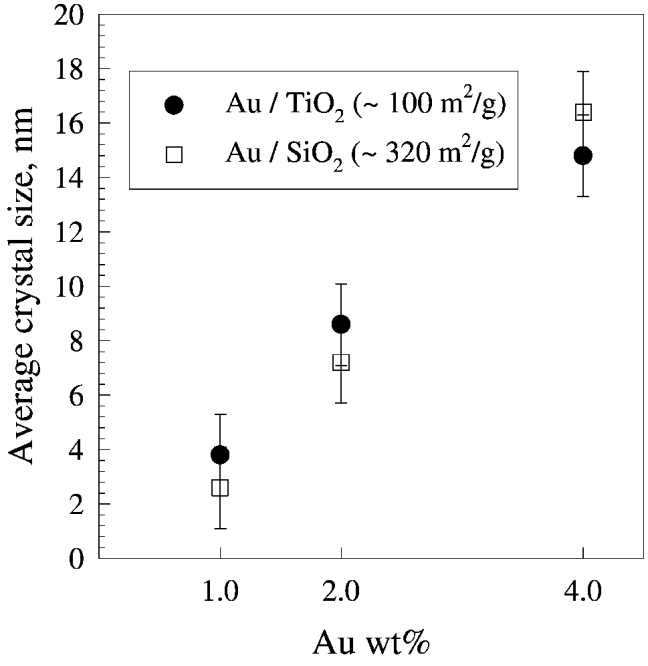

FIG. 8. Average gold crystallite size on titania and silica for 1, 2, and 4 wt% gold. The gold nanoparticles are similar in size despite the fact that the support specific surface area differs more than a factor of 3.

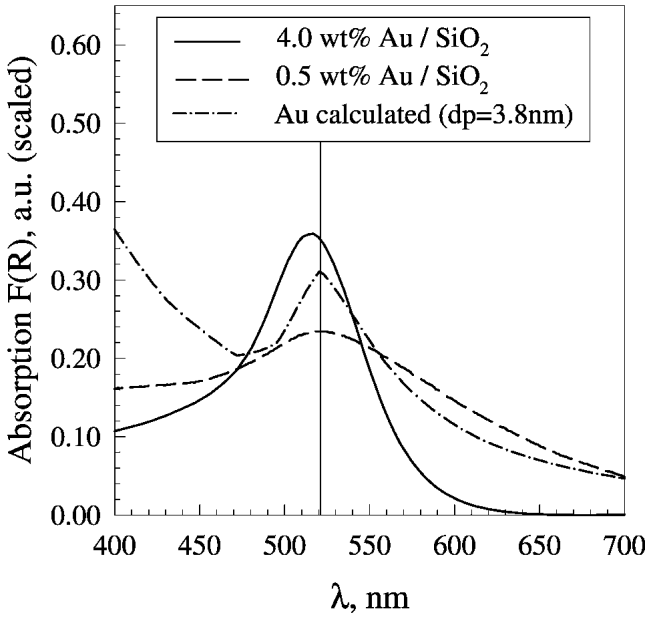

FIG. 10. Gold plasmon peak position for 0.5 and 4 wt% Au/SiO_2 and pure gold (calculated). Only the titania support (Fig. 9) shows a red shift, indicating an interaction between the gold and the metal oxide support.

Spray-flame-made gold particles in this study are nonagglomerated and mostly single crystalline. The steep temperature gradient in the flame creates a highly supersaturated gold vapor. The gold particles may be formed by heterogeneous nucleation on the existing metal oxide support or by homogeneous nucleation of the gold itself. Since the gold particle size is independent of the metal oxide (titania or silica) and independent of the support surface area (100 m^2/g or 320 m^2/g; Fig. 8 at equal Au concentrations) these particles should be formed homogeneously. Barnes *et al.*[20] found that homogeneous nucleation was the major formation mechanism of stable gold particles during hot filament chemical vapor deposition.[20] There, gold particles were formed before deposition on the substrate. Cooling rates in the spray flame are very high and super-cooling of the gold vapor leads to nucleation of gold particles. In fact, coagulation and sintering can not be the dominating mechanisms as increasing the gold concentration (v_m) by a factor of 2 also increased the Au particle size by a factor of 2 and not by $v_m^{2/5} = 2^{2/5}$ as would be expected by coagulation–coalescence in the free molecular regime (Fig. 8).[21] Furthermore, the measured size distribution of Au particles was narrower than that of the self-preserving distribution for particles made by coagulation, supporting further that the latter was not a dominant particle growth mechanism as with titania or silica.[5]

After formation, the gold particles deposit on the metal oxide support without influencing its crystal structure, as was shown with titania (Fig. 3). Furthermore, the formation of the gold clusters does not influence the final specific surface area of the metal oxide support, which emphasizes that the oxides (titania or silica) were formed first. The highly mobile gold particles deposit very efficiently onto the large surface area of the support as the XRD-determined Au content matches its nominal content from the FSP feed. After deposition, the gold interacts weakly with the support. In the case of titania, a small red shift (18 nm) of the surface plasmon band occurred in the absorption spectra. A similar red shift (15 nm) was reported in Au/TiO_2 nanoparticle sols where the gold nanoparticles were deposited on the existing titania particles.[22] In the case of silica, no shift was observed (Fig. 10) because the interaction between the gold and the amorphous and electronically rather inert silica support is weak, which was also reported for wet-phase-made gold-silica core-shell particles.[23] These results show that the Au/oxide particles made by the one-step FSP process behave essentially as the conventionally prepared ones.

V. SUMMARY

A one-step synthesis of Au/TiO_2 or Au/SiO_2 particles by an aerosol flame process resulted in nonagglomerated, well-dispersed, crystalline gold nanoparticles with well-controlled average diameter by the Au precursor concentration. The final gold particle size was independent of the support and its specific surface area, indicating that Au particles follow a formation pathway (nucleation) separate from that of the metal oxide support (coagulation and sintering). Even on silica, gold clusters were well dispersed. Flame-made Au oxide particles exhibited the same UV-vis spectra as wet-chemistry-made ones, indicating the potential of flame technology for manufacture of oxide-supported metal nanoparticles.

ACKNOWLEDGMENTS

The research was supported by the Swiss National Science Foundation, Grant No. 2100-063632.00/1, TH Gesuch 19/01-1 and Kommission für Technologie und Innovation (KTI) TOP NANO 21, Grant No. 5978.2, Switzerland. We gratefully acknowledge the technical support of Dr. F. Krumeich who provided the HRTEM facilities. Stimulating discussions with Prof. A. Baiker (ETH Zurich) are gratefully acknowledged.

REFERENCES

1. P. Moriarty, Rep. Prog. Phys. **64,** 297 (2001).
2. G.C. Bond, Catal. Today **72,** 5 (2002).
3. G.J. Hutchings, Catal. Today **72,** 11 (2002).
4. M. Haruta, Catal. Today **36,** 153 (1997).
5. S.E. Pratsinis, Prog. Energy Combust. Sci. **24,** 197 (1998).
6. M.H. Magnusson, K. Deppert, J.O. Malm, J.O. Bovin, and L. Samuelson, J. Nanoparticle Res. **1,** 243 (1999).
7. K. Nakaso, M. Shimada, K. Okuyama, and K. Deppert, J. Aerosol Sci. **33,** 1061 (2002).
8. T. Johannessen and S. Koutsopoulos, J. Catal. **205,** 404 (2002).
9. H.K. Kammler, L. Mädler, and S.E. Pratsinis, Chem. Eng. Technol. **24,** 583 (2001).
10. M. Sokolowski, A. Sokolowska, A. Michalski, and B. Gokieli, J. Aerosol Sci. **8,** 219 (1977).
11. R.M. Laine, R. Baranwal, T. Hinklin, D. Treadwell, A. Sutorik, C. Bickmore, K. Waldner, and S.S. Neo, Key Eng. Mater. **159–160,** 17 (1999).
12. W.J. Stark, S.E. Pratsinis, and A. Baiker, J. Catal. **203,** 516 (2001).
13. L. Mädler, H.K. Kammler, R. Mueller, and S.E. Pratsinis, J. Aerosol Sci. **33,** 369 (2002).
14. L. Mädler, W.J. Stark, and S.E. Pratsinis, J. Mater. Res. **17,** 1356 (2002).
15. R.W. Cheary and A.A. Coelho, J. Appl. Crystallogr. **31,** 851 (1998).
16. W.C. Hinds, *Aerosol Technology,* 2nd ed. (John Wiley & Sons, Inc., New York, 1999).
17. J. Turkevich, G. Garton, and P.C. Stevenson, J. Colloid Sci. Suppl. **1,** S26 (1954).
18. C.F. Bohren and D.R. Huffman, *Absorption and Scattering of Light by Small Particles,* 1st paperback ed. (John Wiley & Sons, New York, 1998).
19. P.B. Johnson and R.W. Christy, Phys. Rev. B **6,** 4370 (1972).
20. M.C. Barnes, D.Y. Kim, H.S. Ahn, C.O. Lee, and N.M. Hwang, J. Cryst. Growth **213,** 83 (2000).
21. W. Koch and S.K. Friedlander, Part. Part. Syst. Charact. **8,** 86 (1991).
22. S.Y. Zhao, S.H. Chen, S.Y. Wang, and Z.L. Quan, J. Colloid Interface Sci. **221,** 161 (2000).
23. L.M. Liz-Marzan, M. Giersig, and P. Mulvaney, Langmuir **12,** 4329 (1996).